Available online at www.sciencedirect.com
ScienceDirect
Diamond & Related Materials 15 (2006) 1868–1877
DIAMOND AND RELATED MATERIALS
www.elsevier.com/locate/diamond

The origin of shallow n-type conductivity in boron-doped diamond with H or S co-doping: Density functional theory study

Yu Cai [a,1], Tianhou Zhang [a], Alfred B. Anderson [a,*], John C. Angus [b], Lubomir N. Kostadinov [c], Titus V. Albu [d]

[a] Department of Chemistry, Case Western Reserve University, Cleveland, OH 44106, USA
[b] Department of Chemical Engineering, Case Western Reserve University, Cleveland, OH 44106, USA
[c] Department of Physical Chemistry, Bulgarian Academy of Sciences, 1113 Sofia, Bulgaria
[d] Department of Chemistry, Box 5055, Tennessee Technological University, Cookeville, TN 38505, USA

Available online 6 October 2006

Abstract

The ionization potentials and the electron affinities of doped diamond were calculated using B3LYP hybrid density functional theory and nanocrystalline cluster models, while taking into account the quantum confinement of the charge carriers. In many cases donor and acceptor levels were created in the middle of the gap between the conduction and valence bands. A possible explanation for the n-type behavior created by co-doping diamond films with boron and sulfur is given in terms of thermally activated electron donation from an SVS (V is vacancy) donor to a BB acceptor band. Both lie deep in the band gap. It is proposed that electrons in the BB acceptor band are mobile charge carriers. It is also proposed that the conversion of boron-doped diamond from p-type conductivity, with hole charge carriers in the top of the valence band, to n-type conductivity, following treatment in a deuterium plasma, may arise from formation of interstitial hydrogen donor levels and B_nH_m acceptor levels that create an acceptor band in which electrons are mobile. Again, both are deep in the band gap of pure diamond. In a prior attempt to explain this n-type behavior, BH_n defects with unrelaxed structures were proposed to be shallow donors to the diamond conduction band. This paper shows that these defects become deep donors when their structures are optimized. Finally, defects created from vacancies with 1 to 4 H in them are shown to be deep donors to the diamond conduction band.

Keywords: Diamond; n-type; Band gap states

1. Introduction

Boron is the only well documented p-type dopant in diamond [1]. There are two well characterized n-type dopants: substitutional nitrogen and substitutional phosphorous with deep donor sites at 1.6 eV and 0.6 eV respectively [2,3]. Other n-type donors are experimentally and theoretically less well characterized.

Sulfur, in combination with boron, has shown evidence of n-type behavior at low B/S ratios, and Mott–Schottky plots indicate that the Fermi level is 1.2 eV above the Fermi level of boron-doped p-type diamond, which implies that the conduction involves band gap states [4,5]. From electrical resistance measurements at temperatures between 200 K and 300 K, activation energies ranging from 0.05 eV to 0.12 eV were determined for several samples [5].

Previous theoretical studies indicated that S [6–12], SB [6–9], and SBS [8] substituting, respectively, for one, two, and three adjacent C atoms form deep 0.5–1.5 eV conduction band donor sites, though an early study predicted that substitutional S forms a shallow 0.15 eV donor site [13]. None of these results matches the observed placement of the Fermi level at the position noted above. Other experiments on sulfur-doped diamond yielded activation energies for n-type conductivity of 0.38 eV [14,15], 0.32 eV [16], 0.33 eV [17], 0.52 eV [18], and 0.39 eV for B and S co-doped diamond [18].

One goal of our theoretical work is to explore complex doping scenarios that may explain the position of the Fermi level and the low activation energy to n-type conductivity in diamond doped with sulfur and boron. The possibility that defect bands

* Corresponding author. Tel.: +1 216 368 5044; fax: +1 216 368 3006.
E-mail address: aba@case.edu (A.B. Anderson).
[1] Current address: Department of Chemical Engineering, University of Virginia, 102 Engineers' Way, PO Box 400741, Charlottesville, VA 22904, United States.

0925-9635/$ - see front matter © 2006 Elsevier B.V. All rights reserved.
doi:10.1016/j.diamond.2006.08.029

within the band gap may account for n-type conductivity will be discussed. The possibility of an impurity band mechanism for these observations has not to our knowledge been considered previously. Results will be given for combinations of S, B, and vacancies (V) substituting for adjacent carbon atoms. One such combination, SVS as a donor and BB as an acceptor, has the correct energies, within the errors of the model, to account for the experimental observations. We postulate that an electron promoted to a BB acceptor orbital is held very weakly in a large orbit because of the lack of coulomb attraction to the uncharged defect center. We further postulated that these large orbitals overlap and form a conduction band and that mobile electrons within this band provide the observed n-type conductivity.

Boron-doped CVD diamond after treatment in a deuterium plasma also shows n-type behavior [19–22]. The measured effective excitation energies ranged from 0.34 eV to 0.23 eV, decreasing as the B content increased [19–22]. Concentrations ranged from 2×10^{17} to 4×10^{19} B atoms per cm^3. Boron clustering in heavily doped, 10^{17} to 10^{21} cm^{-3}, polycrystalline diamond was proposed previously to account for the electrical deactivation of p-type boron-doped films [23]. BB and BV were suggested as cluster defects and it was concluded: "for boron concentrations exceeding 10^{17} cm^{-1}, acceptor levels are strongly interacting" [23]. A study of diamond doped with boron at the 2×10^{19} to 4×10^{20} cm^{-3} level and exposed to a deuterium plasma showed that B–D complexes are bound by 2.5 eV with respect to dissociated interstitial D^+ and substitutional B^- [24]. Interestingly, measured temperature dependence of deuterium profiles indicated other boron-associated defects trapped deuterium more strongly than B(s), and these were postulated to be pairs of adjacent B(s), i.e. BB defects [24]. Electrical measurements were not reported in Ref. [24].

The cause of the n-type behavior reported in Refs. [19–22] is not completely understood even though several theoretical studies investigated possible explanations of this phenomenon. In a hybrid density functional study using a cluster model with

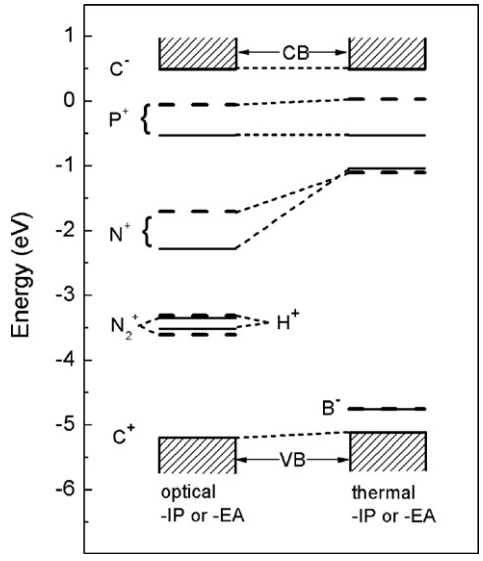

Fig. 1. Calculated energy levels (solid lines) and experimentally determined energy levels (dashed lines) from data tabulated in Ref. [9].

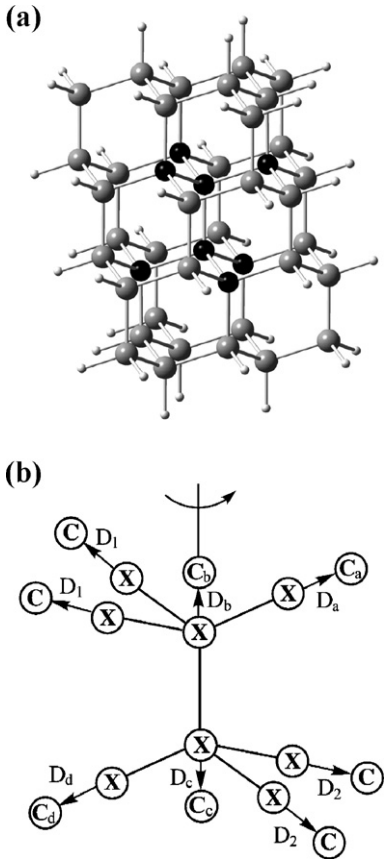

Fig. 2. Cluster model used in this study with defect site atoms in black and structure variable optimized by motions along the [111] directions. The X's indicate positions of dummy atoms used to define the directions of relaxations during structure optimizations. Sp^3 hybridization of surface carbon atoms is maintained by bonding hydrogen atoms (small spheres) to them.

structure constraints, both BH_2 and BH_3 complexes had highest occupied (donor) molecular orbital (HOMO) energy levels that were assigned to be approximately 1.2 and 0.7 eV, respectively, below the lowest unoccupied (acceptor) (LUMO) molecular orbital that was assumed to be the conduction band minimum [25]. Although these results seem to qualitatively explain the experimental observation, Ref. [25] also reported an acceptor level for the BH defect that was shallower than for isolated boron. Such an acceptor would contradict the experimental observation that H passivates p-type boron-doped diamond [22] and with theory demonstrating the passivation [26–29]. Subsequent ab initio studies of BH_n complexes with substitution boron and associated interstitial hydrogen, yielded evidence for deep donor behavior [11,30,31]. We also address these unexpected results and explicitly show that they are caused by the structure constraints used in Ref. [25]. When the constraints are released, the BH_2 and BH_3 defects become, within the donor–acceptor cluster molecular orbital model of Ref. [25], deep donors.

A second goal of the present study is to make an extensive theoretical investigation of the BH_n, BBH_n, and $BBBH_n$ defects, where n ranges from 1 to 3, by including defect structure relaxations, in an attempt to account for the n-type behavior of B- and H-doped diamond. It is found that, within the errors of the

Table 1
−IP(for positive species) or −EA(for negative species) of carbon clusters and clusters with defects containing boron and sulfur

Ionization product	−IP(eV)[a] or −EA (eV)[a]	
	Optical	Thermal
C^-	0.49	0.49
S^+	−1.45	−1.02
BS^+	−1.30	−1.00
SCB^+	−1.73	−1.32
SBS^+	−1.39	−1.27
$BSSB^+$	−3.05	−2.78
BHS^+	−3.33	−2.87
BB^-	−2.53	−3.29
SVS^+	−3.99	−3.79
B^-	−4.21	−4.75
C^+	−5.20	−5.12

A quantum confinement correction is applied for C^-, BB^-, B^-, and C^+ defects. C^-, B^-, and C^+ are from Ref. [9]. H is interstitial and others are substitutional as in Fig. 2.

[a] Energies are measured with respect to the vacuum level.

model, a BBB substitutional defect with a bridging interstitial H atom, BBHB, comes close to having the needed acceptor properties when interstitial H is the donor. It is postulated that the B_3H, or other defects comprised of substitutional boron and interstitial hydrogen atoms, are acceptors that can form a conduction band for mobile electrons in the same way as the BB substitutional pair.

2. Theoretical method

For the structure optimizations and total energy calculations, the Gaussian 03 [32] quantum chemical package was used. It has been shown by Albu et al. [9] that ionization potentials, IP, and electron affinities, EA, calculated by the B3LYP hybrid density functional method with a 6-31G basis set for cluster models of point defects can be used to obtain accurate excitation energy predictions for defects in bulk diamond. This is an alternative to the familiar predictive approach using orbital energy levels via Koopmans' theorem, and as shown below, it is quite accurate. Our predictions use total energy differences from all-electron calculations for the neutral and ionized systems. Using data tabulated in Ref. [9], comparisons between predictions and experimental values from the literature are shown in Fig. 1. Optical values are found experimentally from optical ionization measurements and theoretically from determining the energy of the neutral system and then holding the structure fixed and variationally determining the energy of the ionized state. Since the reference energy of the free electron is 0 eV, the energy levels in the figure are the negative of the EA for acceptor defects and the negative of the IP for donor defects. Thermal values are found experimentally from the temperature dependence of electrical conductivity and theoretically by variationally relaxing the structure upon ionization and determining the energy of the ionized state. Structure data for the results in Fig. 1 are tabulated in Ref. [9]. The cluster and geometry variables used in Ref. [9] are also used in this paper, and are illustrated in Fig. 2. In cases where the electron or hole added to the cluster model is free, the quantum confinement energy, which is the kinetic energy for an electron or hole in a three-dimensional box approximately the size of the cluster model is determined. For the $C_{44}H_{42}$ cluster used, the quantum confinement energy is 2.07 eV [9], and this value is added to the electron affinity of the cluster and subtracted from the ionization potential of the cluster to give the estimate of the bulk properties. This procedure was used to determine the valence and conduction band edges in Ref. [9]. The band gap, E_g, is given by $E_g = IP - EA$, which from the results in Table 1 is $5.12 + 0.49 = 5.61$ eV, which is close to the measured value of 5.49 eV. The quantum confinement energy is also used in cases where the electron is not necessarily in a conduction band, but is in a large orbital weakly held to the defect center. Such should be the case for substitutional B, an acceptor for which there is only a weak electron pairing energy and no net coulomb potential to hold the added electron to the defect center. Thus, increasing the electron affinity of the $C_{43}BH_{42}$ model for interstitial boron by 2.07 eV puts the acceptor level 0.37 eV above the valence band, in agreement with the 0.37 eV measured value. Other predictions are less accurate, and the largest error of the seven predicted values is 0.58 eV for the thermal excitation energy of the substitutional P donor. In support of the quantum confinement model, it is noted that the boron acceptor levels are strongly interacting [23] and the Bohr diameter of B^- in diamond has been estimated to be 17.28 Å [33]; the dimensions of the $C_{44}H_{42}$ cluster are smaller, $9.2 \times 9.6 \times 9.6$ Å [9]. Thus, the unconfined B^- electron orbital is larger than the cluster model, so increasing the electron affinity of B by an energy of electron confinement is reasonable. For another cluster example and further discussion, see Ref. [9].

Fig. 2a shows in black the atoms that were allowed to move in the structure optimizations. Motions in the [111] directions were permitted, as shown in Fig. 2b. In cases of three and four substitutional atoms, the additional atoms were connected to form chains of 3 or 4 substituting atoms. The X's in Fig. 2b are fixed reference points used to define the [111] directions for the calculations. To summarize the notation appearing in the tables

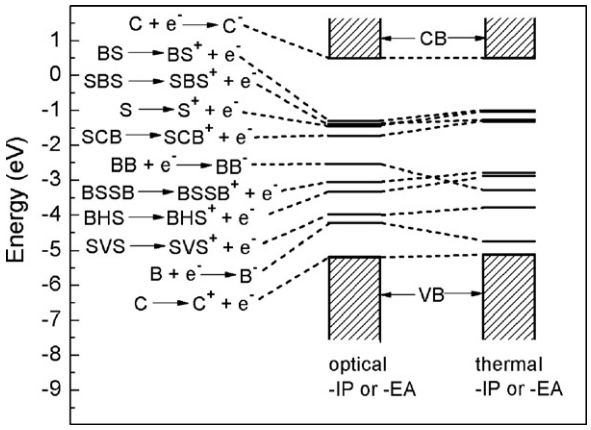

Fig. 3. Calculated optical and thermal −IP and −EA for various diamond clusters with both boron and sulfur dopants. The ionization products are shown on the left. CB is the conduction band and VB is the valence band of bulk diamond.

Table 2
Structure parameters for defects in Table 1 as defined in Fig. 2b

Defect	Charge	Formula	b	D_b	D_1	c	D_c	D_2	a	D_a	R_{bH1}	R_{cH1}
S	0	$C_{43}SH_{42}$	S	0.297	0.251	C	0.168	0.025				
	1	$C_{43}SH_{42}^{+1}$	S	0.068	0.195	C	0.351	0.046				
BS	0	$C_{42}BSH_{42}$	S	0.044	0.255	B	0.186	0.070				
	1	$C_{42}BSH_{42}^{+1}$	S	−0.027	0.188	B	0.236	0.076				
SCB	0	$C_{42}BSH_{42}$	C	0.139	0.039	S	0.071	0.265	B	0.053		
	1	$C_{42}BSH_{42}^{+1}$	C	0.198	0.051	S	−0.024	0.193	B	0.068		
BSSB	0	$C_{40}B_2S_2H_{42}$	S	0.325	0.221	S	0.325	0.221	B	0.255		
	1	$C_{40}B_2S_2H_{42}^{+1}$	S	0.269	0.225	S	0.269	0.225	B	0.262		
BHS	0	$C_{42}BSH_{43}$	S	0.506	0.256	B	0.371	0.085			1.363	1.059
	1	$C_{42}BSH_{43}^{+1}$	S	0.351	0.246	B	0.494	0.087			1.290	1.100
BB	0	$C_{42}B_2H_{42}$	B	0.279	0.057	B	0.279	0.057				
	−1	$C_{42}B_2H_{42}^{-1}$	B	0.121	0.055	B	0.121	0.055				
SVS	0	$C_{41}S_2H_{42}$	V		0.109	S	−0.168	0.164	S	−0.339		
	1	$C_{41}S_2H_{42}^{+1}$	V		0.152	S	−0.083	0.178	S	−0.335		
B	0	$C_{43}BH_{42}$	B	0.120	0.054	C	0.115	0.020				
	−1	$C_{43}BH_{42}^{-1}$	B	0.005	0.049	C	0.030	0.019				

D is displacement from lattice sites and *R* is internuclear distance.

and figures, C represents the bulk diamond cluster, B represents the cluster with boron substituting for a carbon atom, BH represents substitutional boron and adjacent interstitial hydrogen, BB represents two substitutional boron atoms, SVS represents two substitutional sulfur atoms with a carbon atom vacancy between them, and so on.

3. Results and discussion

3.1. BB, SVS, and (B,S) co-doped complexes

Finding a shallow donor complex based on B and S seems unlikely, considering the past theoretical results [6–12]. A number of new defects involving substitutional B and S were tried nevertheless, and the electronic structure results for them and previous calculations are shown in Fig. 3. In one case H was inserted into the BS bond. Ionization energy data for these and other defects are given in Table 1 and their structures before and after ionization are in Table 2. Focusing on the adiabatic results, since they allow for relaxations that occur when thermal occupation of excited states follows the Boltzmann distribution, two calculated acceptors are B and BB. At 0.37 eV above the valence band, B is a relatively shallow acceptor while BB is calculated to be 1.83 eV above, making it a deep acceptor with respect to the valence band. Based on a density functional band calculation, BB has recently been proposed by others to be a deeper acceptor than a single substitutional B [34]. All of the donors except one lie above the B and BB acceptors and are predicted to compensate them. We calculate the BB defect to be 2.09 eV more stable than two isolated substitutional B, while the band calculation in Ref. [34] yielded 0.8 eV for the stability.

The SVS donor defect, which is comprised of two substitutional S atoms on either side of a vacancy, falls 0.50 eV below the BB acceptor level. We suggest that this pair of donor and acceptor defects may, within the uncertainty of the model, be responsible for the conductivity associated with the 0.05 eV to 0.12 eV activation energies observed in Ref. [5]. The Fermi level for this pair is 1.40 eV above the Fermi level for p-type boron-doped diamond. Within the uncertainty of the model, this is in agreement with the 1.2 eV value for the Fermi level position, estimated from Mott–Schottky analysis [4].

Some of the structural details of the defects are of special note. The diamond cluster with the BB defect is shown in Fig. 4. The long 2.10 Å distance between two boron atoms is the result

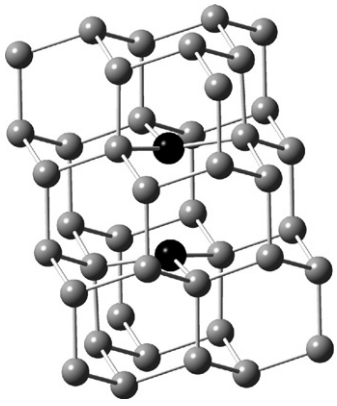

Fig. 4. $C_{42}B_2H_{42}$ cluster model for the defect with two substitutional B atoms. Terminal H are not shown.

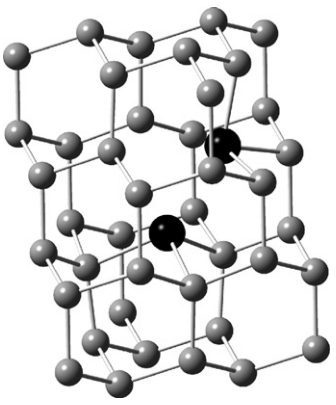

Fig. 5. $C_{41}S_2H_{42}$ cluster model for the defect with two substitutional S atoms and a vacancy site. Terminal H are not shown.

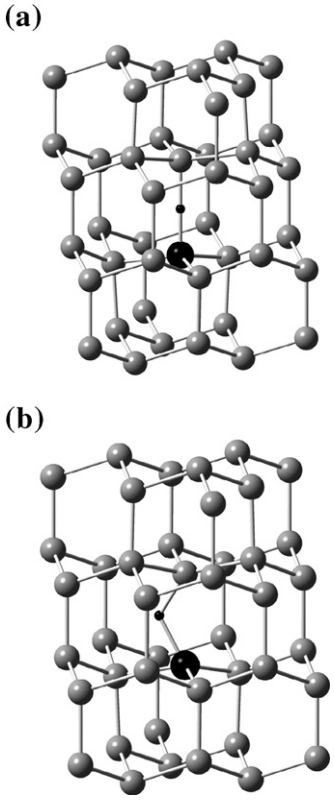

Fig. 6. $C_{43}BHH_{42}$ optimized structure: (a) BH complex with H in the bond-inserted position; (b) BH complex with H in the off-axis site. Terminal H are not shown.

of the zero bond order, i. e., the σ orbital between them is empty. Theoretical results reported in Ref. [24] yielded 1.94 Å for this distance. The SVS structure (Fig. 5) has a vacancy site adjacent to the sulfur atoms. This defect has two S lone-pair orbitals directed into the vacancy, giving the vacancy four electrons and making it isovalent to a carbon atom in the vacancy site. The distance between two sulfur atoms is short at 2.11 Å because the S atoms move part way into the vacancy site.

The stabilities of the defects are worthy of mention. In all of our calculations structures were variationally optimized along the directions defined in Fig. 2. First of all, the isolated vacancy and substitutional B, and S defects are calculated to be thermodynamically very unstable, relative to free atoms. It is calculated to take 15.24 eV to remove a C atom from the $C_{44}H_{42}$ cluster to make a vacancy, and a boron atom bonds to the vacancy site by 11.63 eV. However, a sulfur atom is 4.53 eV unstable when placed in the vacancy site. Thus, substitutional boron atoms can become kinetically trapped in the lattice during the growth, but such trapping would appear less probable for sulfur atoms. However, two substitutional sulfur atoms are greatly stabilized, by 18.86 eV, when sharing a vacancy between them. Sulfur defects in diamond are therefore likely to be associated with vacancies. Two isolated substitutional boron atoms are calculated to become 2.09 eV more stable as BB, which suggests that the formation of BB also is possible during low-pressure diamond growth. However, the kinetic factors for all such reactions are unknown.

The formation of the SVS defect is used to illustrate how the above energies are calculated. The energy change for the process

$$2S + V \rightarrow SVS \tag{1}$$

is given by the reaction energy

$$\begin{aligned}\Delta E &= E(C_{41}SVSH_{42}) \\ &\quad + 2E(C_{44}H_{42}) - 2E(C_{43}SH_{42}) - E(C_{43}VH_{42}) \\ &= -18.86\text{eV}\end{aligned} \tag{2}$$

where the E is calculated total energies of the clusters with the variables shown in Fig. 2 optimized.

3.2. BH_n, B_nH_m, and vacancy complexes co-doped with H

3.2.1. BH_n

In the case of the BH defect, previous workers [26–29] found that interstitial hydrogen is most stable when inserted in a B–C bond. This is due to the electron deficiency of B relative to C which results in a trigonal distortion due to stretching of a B–C bond with a half-filled σ orbital. The H atom's orbital mixes with this half-filled orbital to form a three-centered σ bond. In the present study, two BH defect structures were examined. The first (Fig. 6a) has the interstitial hydrogen in the bond-inserted site, i.e., the B–H–C angle is 180°. The bond lengths B–H and H–C are 1.152 Å and 1.003 Å respectively. For the second one (Fig. 6b), H was not constrained in the B–C bond axis during the structure optimization, and at the optimized B–H–C angle of 119°, the defect is 0.18 eV more stable. The bond lengths of B–H and H–C increased slightly to 1.174 Å and 1.081 Å, respectively. Full structural data for the BH_n complexes may be seen in Table 3. The dissociation energy of the B–H defect has

Table 3
Structure parameters for the neutral and charged complexes BH_n complexes shown in Figs. 6–8

Defect	Charge	Formula	b	D_b	D_1	c	D_c	D_2	R_{bH1}	R_{cH1}	R_{bH2}	R_{cH2}	R_{bH3}	R_{cH3}
BH	0	$C_{43}BH_{43}$	B	0.163	0.046	C	0.163	0.046	1.174	1.081				
	−1	$C_{43}BH_{43}^{-1}$	B	0.218	0.071	C	0.155	0.047	1.174	1.090				
	1	$C_{43}BH_{43}^{+1}$	B	0.270	0.073	C	0.182	0.040	1.212	1.154				
BH_2	0	$C_{43}BH_{44}$	B	0.292	0.096	C	0.212	0.047	1.182	1.564	1.178	1.055		
	−1	$C_{43}BH_{44}^{-1}$	B	0.488	0.104	C	0.238	0.043	1.066	1.540	1.261	1.010		
	1	$C_{43}BH_{44}^{+1}$	B	0.057	0.093	C	0.131	0.051	1.157	1.240	1.166	1.150		
BH_3	0	$C_{43}BH_{45}$	B	0.330	0.111	C	0.248	0.049	1.183	1.304	1.184	1.552	1.175	1.004
	1	$C_{43}BH_{45}^{+1}$	B	0.310	0.130	C	0.230	0.053	1.180	1.171	1.219	1.105	1.137	1.551

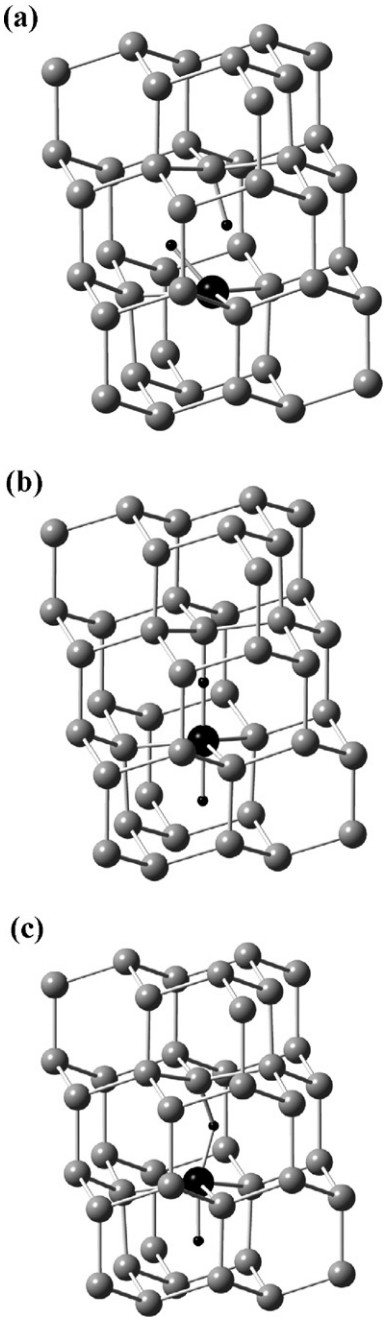

Fig. 7. $C_{43}BH_{44}$ optimized structure: (a) BH_2 complex with two H's in the cis-configuration; (b) BH_2 complex with two H's in the trans configuration, H–B–H–C collinear; (c) BH_2 complex with two H's in the trans configuration, H–B–H–C nonlinear. Terminal H are not shown.

been determined from temperature-dependence measurements of deuterium diffusion profiles to be 2.5±0.2 eV [24]. We calculate 3.24 eV for the dissociation reaction of B–H forming substitutional B^- and interstitial H^+. A density functional band study in Ref. [24] obtained 2.7 eV for this process and a density functional cluster study reported 3.8 eV in Ref. [11].

For the BH_2 complex, three structures were considered. The first one (Fig. 7a) has two interstitial hydrogen atoms on one side of the boron. Two well-defined bonds can be seen in Fig. 7a, 1.151 Å for B–H and 1.066 Å for C–H. The second structure

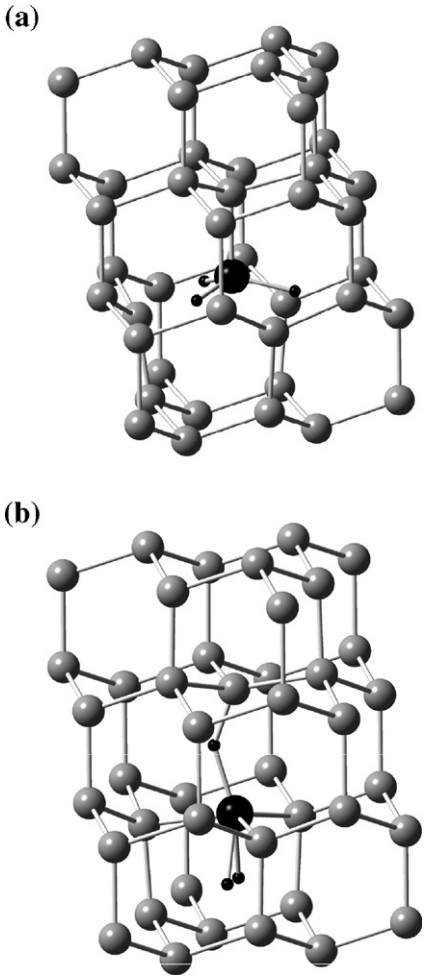

Fig. 8. $C_{43}BH_{45}$ optimized structure: (a) BH_3 complex with C_{3v} symmetry constraint; (b) BH_3 complex with no symmetry. Terminal H are not shown.

(Fig. 7b) is 0.07 eV more stable and has one H inserted in the BC bond and the other in the so-called "antibonding" position on the other side of B, both lying on the B–C bond axis. The third, and most stable BH_2 structure, is a distorted version of this, the two H atoms having relaxed off the B–C axis, as shown in Fig. 7c. This structure is 0.13 eV more stable than the first structure.

Table 4
Reaction energies, ΔE (eV), for several processes involving addition of hydrogen to clusters containing boron

Reactions[a]	B+H→BH	BH+H→BH_2	BH_2+H→BH_3
ΔE (eV)	−4.66	0.53	−1.79
Reactions[b]	BB+H→BHB	BHB+H→BHHB	BHHB+H→BHHBH
ΔE (eV)	−3.44	−4.23	0.72
Reactions[c]	BBB+H→BHBB	BHBB+H→BHHBB	BHHBB+H→BHHBHB
ΔE (eV)	−5.36	−3.19	−3.84

A positive ΔE indicates that the product is less stable than the reactants.
[a] B refers to cluster $C_{43}BH_{42}$.
[b] BB refers to cluster $C_{42}B_2H_{42}$; the first two H atoms bridge the BB pair and third is in an "antibonding" site.
[c] BBB refers to cluster $C_{41}B_3H_{42}$; the H atoms bridge the BB pairs in the order shown.

According to Ref. [25], the most stable BH_3 complex has C_{3v} symmetry with three interstitial hydrogen atoms lying along [001] directions. With this symmetry constraint, a similar local minimum structure was found in our calculations (Fig. 8a) with B–H bond lengths of 1.135 Å. However, upon relaxing the geometry constraints, and giving the three hydrogen atoms all degrees of freedom, a 3.76 eV more stable structure was found, with one hydrogen atom inserted off axis in the B–C bond and other two in the antibonding position (Fig. 8b). The distance between two hydrogen atoms in the antibonding position is 0.702 Å, which is slightly less than the equilibrium bond length in a hydrogen molecule, 0.74142 Å [35].

Hydrogenation stabilization energies ΔE for forming the BH_n defects according to reactions of the form

$$BH_n + H \rightarrow BH_{n+1} \quad (3)$$

were calculated using the equation

$$\Delta E_{n+1} = E(C_{43}BH_{n+1}H_{42}) + E(C_{44}H_{42}) - E(C_{43}BH_nH_{42}) - E(C_{43}CHH_{42}) \quad (4)$$

As shown in Table 4, BH is 4.66 eV more stable than the combination of isolated B and H_i defects, but subsequent stepwise additions of H to form BH_2 and BH_3 defects by Eq. (3) are endothermic by 0.53 eV and exothermic by 1.79 eV, respectively. This means that BH_2 and BH_3 defects are less likely to form during growth, and if some do form, annealing may dissociate them. A similar conclusion was reached in the theoretical study in Ref. [15].

The calculated −IP and −EA for several of the BH_n defects along with other species are tabulated in Table 5. Focusing on the thermal or adiabatic ionization potentials, which relate to the generation of thermally-induced electron charge carriers in the conduction band, it is seen that BH, BH_2 and BH_3 are all very deep donors to the conduction band. BH is isovalent to C, which explains why its IP is so large. BH_2 is a mid-band gap donor, the lesser value for the IP being in part due to the unpaired electron. BH_3 is closed-shell, so its IP is larger than that for BH_2, but smaller than for BH. Thus BH_2 and BH_3 are predicted to be unstable and very deep donors.

We examine the donor properties of BH_3 because of the recent theoretical interest in it [11,25,30,31]. Using the same C_{3v} geometry constraint as in Ref. [16], the BH_3 donor level moves to a position 2.60 eV higher than we calculated for the optimized structure, placing it closer to the conduction band, as shown in Table 5. This is somewhat similar to the conclusion in Ref. [25] that was based on orbital energy levels alone, using Koopmans' theorem, that were obtained from constrained symmetry calculations for a smaller cluster. When we apply the same structure constraint in our calculations, the HOMO energy rises 4.03 eV from −4.68 eV to −0.65 eV, placing it just 0.55 eV above the LUMO. The 0.55 eV difference in energy levels is quite close to the energy difference reported in Ref. [25]. However, when we use the much more stable optimized structure, the HOMO lies at −4.68 eV and the LUMO lies at 1.49 eV for a separation of 6.17 eV. Therefore, it may be concluded that the closeness of the HOMO and LUMO orbital energy levels reported in Ref. [25] was due to the structure constraint. Refs. [11,30,31] also argued for deep donor behavior of BH_3.

Table 5
−IP(for positive species) or −EA(for negative species) of carbon clusters and clusters with defects containing boron and hydrogen

Ionization product	–IP(eV)[a] or –EA (eV)[a]	
	Optical	Thermal
BH^-	0.54	0.51
C^-	0.49	0.49
$BHHB^-$	0.05	−0.11
$BHHHB^-$	−0.16	−0.12
$BHHBHB^-$	−0.75	−0.83
BH_3^+, C_{3v}	−1.91	−1.69
$BHHBH^-$	−0.78	−2.04
BH_2^+	−4.64	−2.63
BB^-	−2.54	−3.29
H^+	−3.35	−3.33
$BHBB^-$	−3.12	−3.72
BBB^-	−3.99	−4.22
BH_3^+	−6.04	−4.29
BHB^-	−4.08	−4.60
B^-	−4.21	−4.75
$BHHBB^-$	−4.52	−4.85
C^+	−5.20	−5.12
BHB^+	−6.63	−6.22
$BHHB^+$	−6.89	−6.73
BH^+	−6.98	−6.96

A quantum confinement correction is applied for C^-, B^-, C^+, BB^-, and B_nH_{im} defects. C^-, H_i^+, B^-, and C^+ are from Ref. [9]. The BH_3^+, C_{3v} entry is for a constrained structure. H is interstitial and the others are substitutional.
[a] Energies are measured with respect to the vacuum level.

3.2.2. B_2H_n and B_3H_m

The calculated ionization potentials for B_2H_n and B_3H_m complexes were always very positive (a few IP are given in Table 5, and structure parameters for these defects are in Table 6); it is unlikely that a shallow donor to the conduction band of diamond will be found for a defect of this composition. However, B is a shallow acceptor from the valence band, BB is a mid-band gap acceptor, and BH, being iso-electronic to C, has its acceptor level high at 0.02 eV above the conduction band edge. It was shown in the previous section that SVS is a mid-band gap donor that can donate to a conduction band formed from the diffuse orbitals of BB defects for which we postulate high electron mobility. We calculate the BBB defect to be stable by 1.70 eV relative to three isolated B defects, so it is a candidate for formation during low pressure growth, though the kinetics are unknown. The conversion of p-type boron-doped diamond to n-type by exposure to deuterium plasma at 450 °C to 550 °C and its partial reversibility on annealing [19–22] suggests that H will passivate the B and BB acceptor sites, since it lies above them in Table 5 and Fig. 9, and, in sufficient quantities, may form H sites that might donate to a B_nH_m acceptor band.

The BB defect can bond one and two H, but not three, as shown in Table 4. The first and second H bond by 3.44 eV and 4.23 eV, respectively, but a third H will not bond. Density

Table 6
Structure parameters for B_nH_m defects

Defect	Charge	Formula	b	D_b	D_1	c	D_c	D_2	a	D_a	R_{bH1}	R_{cH1}	R_{aH1}	R_{bH2}	R_{cH2}	R_{bH3}	R_{aH3}
B_2H_2	0	$C_{42}B_2H_{44}$	B	0.180	0.086	B	0.179	0.085			1.258	1.207		1.206	1.260		
	−1	$C_{42}B_2H_{44}^{-1}$	B	0.140	0.093	B	0.139	0.093			1.245	1.207		1.209	1.248		
B_2H_3	0	$C_{42}B_2H_{45}$	B	0.186	0.092	B	0.162	0.102			1.228	1.272		1.226	1.272	1.761	1.420
	−1	$C_{42}B_2H_{45}^{-1}$	B	0.170	0.080	B	0.129	0.122			1.214	1.200		1.398	1.231	1.738	1.371
B_3H_3	0	$C_{41}B_3H_{45}$	B	0.058	0.080	B	0.175	0.087	B	0.191	1.155	1.363	1.468	1.225	1.225	1.163	1.224
	−1	$C_{41}B_3H_{45}^{-1}$	B	0.057	0.090	B	0.180	0.089	B	0.197	1.146	1.416	1.423	1.183	1.196	1.143	1.248
H	0	$C_{44}H_{43}$	C	0.328	0.047	C	0.328	0.047									
	1	$C_{44}H_{43}^{+1}$	C	0.298	0.050	C	0.298	0.050									
B_3H	0	$C_{41}B_3H_{43}$	B	0.299	0.054	B	0.275	0.061	B	0.236	1.145	1.629	1.314				
	−1	$C_{41}B_3H_{43}^{-1}$	B	0.181	0.055	B	0.157	0.065	B	0.196	1.132	1.295	1.515				
B_2H	0	$C_{42}B_2H_{43}$	B	0.221	0.074	B	0.222	0.073			1.200	1.225					
	−1	$C_{42}B_2H_{43}^{-1}$	B	0.176	0.072	B	0.179	0.072			1.115	1.121					
B_3H_2	0	$C_{41}B_3H_{44}$	B	0.222	0.073	B	0.218	0.079	B	0.205	1.143	1.599	1.269	1.259	1.227		
	−1	$C_{41}B_3H_{44}^{-1}$	B	0.152	0.074	B	0.178	0.077	B	0.173	1.130	1.574	1.236	1.150	1.174		
B_2H	0	$C_{42}B_2H_{43}$	B	0.221	0.074	B	0.222	0.073			1.200	1.225					
	−1	$C_{42}B_2H_{43}^{-1}$	B	0.176	0.072	B	0.179	0.072			1.115	1.121					
	1	$C_{42}B_2H_{43}^{+1}$	B	0.319	0.073	B	0.293	0.065			1.265	1.493					
B_2H_2	0	$C_{42}B_2H_{44}$	B	0.180	0.086	B	0.179	0.085			1.258	1.207		1.206	1.260		
	−1	$C_{42}B_2H_{44}^{-1}$	B	0.140	0.093	B	0.139	0.093			1.245	1.207		1.209	1.248		
	1	$C_{42}B_2H_{44}^{+1}$	B	0.236	0.085	B	0.235	0.085			1.354	1.238		1.238	1.346		

functional band calculations in Ref. [24] yielded 3.8 eV for bonding one interstitial H atom to BB. Our calculations predict that the BBB defect can bond at least three H, also shown in Table 4. The first H bonds most strongly to BBB, by 5.36 eV. This is the strongest of all calculated interactions between H and B_nH_m defects examined thus far and suggests that this defect might form during low pressure diamond growth. As seen in Table 5 and Fig. 9, BHBB is a mid-band gap acceptor, though it is 0.39 eV below the H donor.

Some general trends are present in the hydrogen affinities and the electron affinities of the BH_n, B_2H_n, and B_3H_n defects. These energies are higher when the defects are radicals, for example, they are higher for B compared to BH, and for B_2H compared to B_2, and for B_3 compared to B_3H, and so on. The differences can be attributed in part to the presence or absence of electron pairing energies. As discussed in Refs. [19–22], the

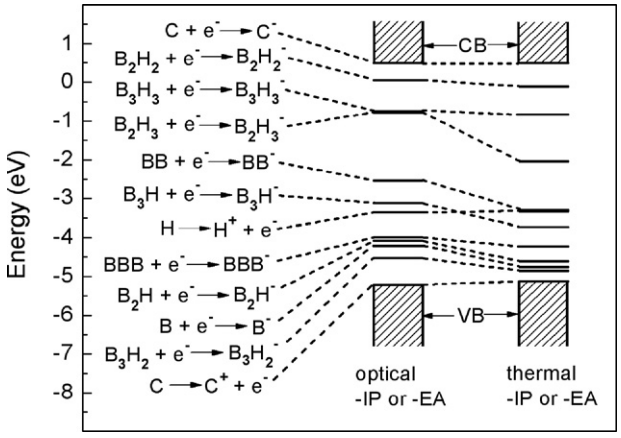

Fig. 9. Calculated optical and thermal −IP/−EA for various diamond clusters with both boron and hydrogen dopants. The ionization products are shown on the left. CB is the conduction band and VB is the valence band of bulk diamond.

incorporation of deuterium into boron-doped diamond by the plasma method seems to go in two stages. During the first step the deuterium passivates the uncompensated B acceptors, and the D/B ratio becomes about 1. The second step leads to n-type conductivity, and the D/B ratio becomes about 2. The charge carrier concentration increases with increased B doping, and the activation energy decreases from 0.34 eV for low B concentrations to a range of 0.25 eV to 0.31 eV for high B concentrations. Based on our model, this lowering of the activation energy can be attributed to the widening of the boron defect-based acceptor band and a smaller contribution from the widening of the H donor band.

3.2.3. VH_n

Earlier theoretical work showed that one to four interstitial H can bond to a carbon vacancy site in diamond, but the donor characteristics were not given [36]. Recent density function band model calculations indicated deep donor behavior for VH_1–VH_4, with respective levels at 1.3, 0.7, 0.6, and −0.2 eV relative to the valence band edge [37]. In Table 7 it may be seen that we predict the H to become very stable when entering a vacancy. This is because interstitial H is unstable by 3.31 eV relative to gas phase H [38], and each of the four carbon atoms surrounding the vacancy is unsaturated and can form a single bond. Steric

Table 7
Calculated reaction energy, ΔE, for adding stepwise one to four interstitial hydrogen atoms to the vacancy diamond cluster $C_{43}H_{42}$, and the thermal ionization potential, −IP

Complex	ΔE (eV)	−Thermal IP (eV)
VH	−8.39	−5.16
VH_2	−6.35	−5.43
VH_3	−6.13	−6.59
VH_4	−5.67	−7.23

crowding causes the exothermicity for forming a bond to decrease as more H atoms are added to the vacancy. We predict that all of the VH_n defects are very deep donors with levels beneath the valence band top. Therefore, even if hydrogen-filled vacancies are present as defects in large quantity, they will not contribute to the n-type behavior discussed in this paper.

4. Concluding comments

Experimentally observed shallow n-type conductivity when diamond is co-doped with boron and sulfur [4,5] is explained in terms of SVS donors and BB acceptors in the band gap. The BB acceptors hold the electrons in orbitals of very large radii because the defects provide no coulomb or electron pairing attraction. With sufficient overlap between sites these orbitals can form a mid-gap conduction band with good electron mobility. Simple estimates indicate that at the maximum boron concentrations, approximately 10^{19} cm^{-3}, the Bohr radii of these defects are close to the average distance between centers, which indicates that orbital overlap is possible in these situations. Further experimental and theoretical characterization of these orbitals is a significant goal. The positive charges (holes) created by electron excitation from the SVS donor sites occupy compact wavefunctions with less overlap between donor sites and so are well localized, with low resulting mobility. These arguments indicate that n-type conduction should dominate in measurements.

For the SVS donor, the excitation energy to the BB acceptor is small, 0.50 eV and in reasonable agreement with measured activation energies in Ref. [4]. The Fermi level lies 1.40 eV above the Fermi level for p-type boron-doped diamond, in satisfactory agreement with the 1.2 eV difference determined from Mott–Schottky analysis in Ref. [4]. Thus it appears that the SVS donor BB acceptor system may account for the n-type conductivity observed in the B/S co-doped diamond films.

The change in boron-doped diamond from p-type conductivity to n-type upon D (H) plasma treatment can be tentatively attributed to states in the band gap where interstitial H is the mid-band gap donor and a B_nH_m complex serves as the mid-band gap acceptor. Of the boron based defects tried, BB would be an excellent acceptor candidate, except it is expected to be passivated by the plasma treatment, just like B. BBHB has nearly the right acceptor property, and if it is present in the original boron-doped diamond or formed from BBB by the plasma treatment it might, within the errors of the calculations, be a shallow acceptor relative to H donors. However, BBHB can bond H and become passivated. As pointed out in Ref. [22], annealing the n-type samples converts them to non-conducting and finally p-type as H diffuses out. Since one or two H_i bond to BB and BBB more strongly than H_i bonds to B it would seem that, once hydrogenated, the BB and BBB defects would be robust toward annealing. This suggests the need for further theoretical studies of new cluster defects and at the same time suggests experiments such as exposing the boron–sulfur-doped n-type diamond to D (H) plasma to see if it eliminates conductivity by passivating BB acceptors and increased exposure of boron-doped systems to the D (H) plasma to see if the proposed BBHB acceptors are passivated. Also, measurement of the barrier voltage of a Schottky junction between boron-doped diamond and D (H) treated boron-doped diamond should provide information on the relative positions of the Fermi levels in the two materials.

Finally, the calculations very strongly suggest that any vacancies that form during low pressure diamond growth will be saturated with H. Such defects will be deep donors.

Acknowledgement

This research is supported by the U. S. National Science Foundation, Grant no. CHE-0314688.

References

[1] K. Thonke, Semicond. Sci. Technol. 18 (2003) S20.
[2] R. Kalish, Carbon 37 (1999) 781.
[3] M. Nesladek, Semicond. Sci. Technol. 20 (2005) R19.
[4] S.C. Eaton, A.B. Anderson, J.C. Angus, Y.E. Evstefeeva, Y.V. Pleskov, Electrochem. Solid-State Lett. 5 (2002) G65.
[5] S.C. Eaton, A.B. Anderson, J.C. Angus, Y.E. Evstefeeva, Y.V. Pleskov, Diamond Relat. Mater. 12 (2003) 1627.
[6] A.B. Anderson, E.J. Grantscharova, J.C. Angus, Phys. Rev., B 54 (1996) 14341.
[7] T. Albu, A.B. Anderson, J.C. Angus, in: G.M. Swain, T. Ando, J.C. Angus, W.D. Brown, J.L. Davidson, A. Gicquel, W.P. Kang, B.V. Spitsyn (Eds.), PV 2001-25, The Electrochemical Society Proceedings Series, Pennington, NJ, 2001.
[8] T. Miyazaki, H. Okushi, Diamond Relat. Mater. 10 (2001) 449.
[9] T.V. Albu, A.B. Anderson, J.C. Angus, J. Electrochem. Soc. 149 (2002) E143.
[10] E.B. Lombardi, A. Mainwood, K. Osuch, Diamond Relat. Mater. 12 (2003) 490.
[11] E.B. Lombardi, A. Mainwood, K. Osuch, Phys. Rev., B 70 (2004) 205201-1.
[12] J.P. Goss, P.R. Briddon, S.J. Sque, R. Jones, Diamond Relat. Mater. 13 (2004) 684.
[13] D. Saada, J. Adler, R. Kalish, Appl. Phys. Lett. 77 (2000) 878.
[14] I. Sakaguchi, M. Nishitani-Gamo, Y. Kukuchi, E. Yasu, H. Haneda, T. Suzuki, T. Ando, Phys. Rev., B 60 (1999) R2139.
[15] M. Nishitani-Gamo, C. Xiao, Y. Zhang, E. Yasu, Y. Kukuchi, I. Sakaguchi, T. Suzuki, Y. Sato, T. Ando, Thin Solid Films 382 (2001) 113.
[16] J.F. Prins, Diamond Relat. Mater. 10 (2001) 1756.
[17] Y.G. Chen, M. Hasegawa, H. Okusi, S. Koizumi, H. Yoshida, T. Sakai, Diamond Relat. Mater. 11 (2002) 451.
[18] R. Li, X. Hu, H. Shen, X. He, Mater. Lett. 58 (2004) 1835.
[19] Z. Teukam, J. Chevallier, C. Saguy, R. Kalish, D. Ballutaud, M. Barbe, F. Jomard, A. Tromson-Carli, C. Cytermann, J.E. Butler, M. Bernard, C. Baron, A. Deneuville, Nat. Mater. 2 (2003) 482.
[20] C. Saguy, R. Kalish, C. Cytemann, Z. Teukam, J. Chevallier, F. Jomard, A. Tromson-Carli, J.E. Butler, C. Baron, A. Deneuville, Diamond Relat. Mater. 13 (2004) 700.
[21] J. Chevallier, Z. Teukam, C. Saguy, R. Kalish, C. Cytermann, F. Jomard, M. Barbe, T. Kociniewski, J.E. Butler, C. Baron, A. Deneuville, Phys. Status Solidi 11 (2004) 2444.
[22] R. Kalish, C. Saguy, C. Cytermann, J. Chevallier, Z. Teukam, F. Jomard, T. Kociniewski, D. Ballutaud, J.E. Butler, C. Baron, A. Deneuville, J. Appl. Phys. 96 (2004) 7060.
[23] D. Narducci, C.R. Guarnieri, J.J. Cuomo, J. Electrochem. Soc. 138 (1991) 2446.
[24] J.P. Goss, P.R. Briddon, R. Jones, Z. Teukam, D. Ballutaud, F. Jomard, J. Chevallier, M. Bernard, A. Deneuville, Phys. Rev., B 68 (2004) 235209-1.
[25] Y. Dai, D. Dai, D. Liu, S. Han, B. Huang, Appl. Phys. Lett. 84 (2004) 1895.
[26] S.P. Mehandru, A.B. Anderson, J. Mater. Res. 9 (1994) 383.

[27] S.J. Breuer, P.R. Briddon, Phys. Rev., B 49 (1994) 10332.
[28] J. Chevallier, B. Theys, A. Lusson, C. Grattepain, A. Deneuville, E. Gheeraert, Phys. Rev., B 58 (1998) 7966.
[29] J.P. Goss, R. Jones, M.I. Heggie, C.P. Ewels, P.R. Briddon, S. Oberg, Phys. Rev., B 65 (2002) 115207-1.
[30] J.P. Goss, P.R. Briddon, S.J. Sque, R. Jones, Phys. Rev., B 69 (2004) 165215-1.
[31] J.P. Goss, P.R. Briddon, R. Sachdeva, R. Jones, S.J. Sque, AIP Conf. Proc., vol. 772, 2005, p. 91.
[32] M.J. Frisch, G.W. Trucks, H.B. Schlegel, G.E. Scuseria, M.A. Robb, J.R. Cheeseman, J.A. Montgomery, T.V. Jr., K.N. Kudin, J.C. Burant, J.M. Millam, S.S. Iyengar, J. Tomasi, V. Barone, B. Mennucci, M. Cossi, G. Scalmani, N. Rega, G.A. Petersson, H. Nakatsuji, M. Hada, M. Ehara, K. Toyota, R. Fukuda, J. Hasegawa, M. Ishida, T. Nakajima, Y. Honda, O. Kitao, H. Nakai, M. Klene, X. Li, J.E. Knox, H.P. Hratchian, J.B. Cross, C. Adamo, J. Jaramillo, R. Gomperts, R.E. Stratmann, O. Yazyev, A.J. Austin, R. Cammi, C. Pomelli, J.W. Ochterski, P.Y. Ayala, K. Morokuma, G.A. Voth, P. Salvador, J.J. Dannenberg, V.G. Zakrzewski, S. Dapprich, A.D. Daniels, M.C. Strain, O. Farkas, D.K. Malick, A.D. Rabuck, K. Raghavachari, J.B. Foresman, J.V. Ortiz, Q. Cui, A.G. Baboul, S. Clifford, J. Cioslowski, B.B. Stefanov, G. Liu, A. Liashenko, P. Piskorz, I. Komaromi, R.L. Martin, D.J. Fox, T. Keith, M.A. Al-Laham, C.Y. Peng, A. Nanayakkara, M. Challacombe, P.M.W. Gill, B. Johnson, W. Chen, M.W. Wong, C. Gonzalez, J.A. Pople, Gaussian 03 Revision C.02, Gaussian Inc., Wallingford, CT, 2004.
[33] E.P. Visser, G.J. Bauhuis, G. Janssen, W. Vollenberg, W.J.P. van Enckevort, L.J. Giling, J. Phys., Condens. Matter 4 (1992) 7365.
[34] J.P. Goss, P.R. Briddon, Phys. Rev., B 73 (2006) 085204-1.
[35] K.P. Huber, G. Herzberg, Molecular Spectra and Molecular Structure IV. Constants of Diatomic Molecules, Van Nostrand Reinhold, New York, N.Y., 1979, p. 270.
[36] S.P. Mehandru, A.B. Anderson, J.C. Angus, J. Mater. Res. 7 (1992) 689.
[37] J.P. Goss, P.R. Briddon, R. Jones, S. Sque, Diamond Relat. Mater. 13 (2004) 684.
[38] A.B. Anderson, L.N. Kostadinov, J.C. Angus, Phys. Rev., B 67 (2003) 233402-1.